Power and Complex Envelope Correlation for Modeling Measured Indoor MIMO Channels: A Beamforming Evaluation

Jon Wallace*, Hüseyin Özcelik†, Markus Herdin†, Ernst Bonek†, and Michael Jensen*

*Department of Electrical and Computer Engineering
Brigham Young University, 459 CB, Provo, UT 84602-4099
Phone: (801)422-5736   Fax: (801)422-0201
Email: jensen@ee.byu.edu

†Institut für Nachrichtentechnik und Hochfrequenztechnik
Technische Universität Wien, Gusshausstrasse 25/389, A-1040 Wien, Austria
Phone: (+43 1) 58801 - 38901   Fax: (+43 1) 58801 - 38999
Email: ernst.bonek@tuwien.ac.at

Abstract— The multivariate complex normal distribution is often employed as a tractable and convenient model for MIMO wireless systems. Several models may result depending on how the covariance matrix is specified, i.e. power or complex envelope correlation and full or separable (Kronecker) correlation. This paper investigates the differences of the various models by applying a joint transmit/receive beamformer to recent wideband MIMO radio channel measurements at 5.2 GHz. It is found that the Kronecker model, especially for power correlation, significantly alters the joint beamformer spectrum. A multipath clustering model is applied whose parameters are estimated directly from the measured data. The clustering model is able to match capacity pdfs, and resulting simulated joint beamformer spectra look more realistic than those generated with conventional separable correlation functions.

I. INTRODUCTION

Early studies of multiple-input multiple-output (MIMO) wireless channels focused on the independent and identically distributed (i.i.d.) complex normal model due to simplicity and the lack of real MIMO channel information [1]. Later studies have considered the effect of spatial correlation [2], [3]. The Kronecker correlation model [4] assumes that the channel covariance matrix is a separable product of transmit and receive covariances, given by either complex or power envelope correlation. Such descriptions are attractive, since previous results from diversity studies may be applied. These models have been validated by comparing the statistics of aggregate metrics, such as channel capacity or channel eigenvalues [5].

Three main deficiencies are evident in previous work in this area. First, although multivariate complex normal models are widely applied, the differences in the various models have received little attention. Second, these statistical models are often presented without any physical interpretation of the channel's multipath behavior. Third, very little mention is made of how to generate realistic covariance matrices, aside from computing them directly from measured data or using possibly over-simplistic correlation functions.

We alleviate these difficulties by applying a simultaneous transmit/receive beamformer to explore the differences between multivariate complex normal MIMO models with either power or complex envelope correlation and either full or separable (Kronecker) covariance. The beamforming approach provides a compelling physical interpretation that demonstrates how the various models influence the multipath structure of the modeled channel. Application of the method to recent wideband indoor MIMO measurements demonstrates how the models may distort the true channel behavior. Finally, we apply a diffuse spectrum estimation technique to obtain parameters for a path-based clustering model. The model generates full covariance matrices, whose simulated channels look more realistic than those generated with simple conventional correlation functions.

II. COMPLEX NORMAL MODELS

Since the purpose of this work is to analyze the various multivariate complex normal MIMO models, a brief treatment of the fundamental distribution and simplifying assumptions is convenient.

A. Complex Normal Distribution

A multivariate complex-normal distributed random vector $\mathbf{x}$ has the probability density function (pdf)

$$f(\mathbf{x}) = \frac{1}{\pi^N |\mathbf{R}|} \exp[-(\mathbf{x} - \boldsymbol{\mu})^H \mathbf{R}^{-1}(\mathbf{x} - \boldsymbol{\mu})], \qquad (1)$$

where $\{\cdot\}^H$ is conjugate transpose, $\mathbf{R}$ is the covariance matrix, N is the dimensionality of $\mathbf{R}$, and $\boldsymbol{\mu}$ is the mean of $\mathbf{x}$. Consider a MIMO system with N_T transmit antennas and N_R receive antennas, whose $N_R \times N_T$ channel matrix $\mathbf{H}$ is composed of zero-mean complex-normal distributed elements. The covariance of the ijth and $k\ell$th elements of $\mathbf{H}$ is

$$R_{ij;k\ell} = \mathrm{E}\{H_{ij}H_{k\ell}^*\}, \qquad (2)$$

where $\mathrm{E}\{\cdot\}$ is expectation. To write $\mathbf{R}$ as a standard covariance matrix, we normally let $\mathbf{h} = \mathrm{Vec}\{\mathbf{H}\}$, where $\mathrm{Vec}\{\cdot\}$ is the vector (or column stacking) operation, and compute $\mathbf{R} = \mathrm{E}\{\mathbf{h}\mathbf{h}^H\}$. This stacking operation is equivalent to defining the row (i') and column (k') indices to be $i' = i + (j-1)N_R$ and $k' = k + (\ell-1)N_R$.

Since the full covariance is an $(N_R N_T) \times (N_R N_T)$ matrix, the number of parameters may be prohibitive from a modeling perspective. Two important simplifying assumptions reduce the number of independent parameters. *Separability* assumes that the full covariance matrix may be written as a product of transmit covariance $(\mathbf{R}_T)$ and receive covariance $(\mathbf{R}_R)$ or $R_{ij,k\ell} = R_{R,ik}R_{T,j\ell}$. For such channels, the transmit and receive covariances can be computed from the full covariances as

$$R_{T,ij} = \frac{1}{\alpha}\sum_{k=1}^{N_R}R_{ki,kj}, \qquad R_{R,ij} = \frac{1}{\beta}\sum_{k=1}^{N_T}R_{ik,jk}, \quad (3)$$

where α and β are chosen such that

$$\alpha\beta = \sum_{k_1=1}^{N_R}\sum_{k_2=1}^{N_T}R_{k_1 k_2, k_1 k_2}. \quad (4)$$

This assumption is equivalent to the Kronecker model, where $\mathbf{R} = \mathbf{R}_R \otimes \mathbf{R}_T$, $\mathbf{R}_R = \alpha^{-1}\mathrm{E}\{\mathbf{H}\mathbf{H}^H\}$, $\mathbf{R}_T^T = \beta^{-1}\mathrm{E}\{\mathbf{H}^H\mathbf{H}\}$, $\alpha = \beta = \left(\mathrm{E}\{\|\mathbf{H}\|_F^2\}\right)^{1/2}$, where $\{\cdot\}^T$ is matrix transpose.

Shift-invariance assumes that the covariance matrix is only a function of antenna displacement (not absolute antenna location) and holds for special array structures such as uniform linear arrays in the presence of far-field scattering. The relationship between the full covariance and shift-invariant covariance $(\mathbf{R}_S)$ is

$$R_{ij,k\ell} = R_{S,i-k,j-\ell}. \quad (5)$$

The combination of separability and shift-invariance allows full covariance matrices to be generated from existing correlation functions such as Jakes' model.

B. Power and Complex Envelope Correlation

A zero-mean multivariate complex-normal distributed vector $\mathbf{x}$ is completely characterized by the covariance matrix $\mathbf{R} = \mathrm{E}\{\mathbf{x}\mathbf{x}^H\}$. We refer to the covariance computation $\mathrm{E}\{\mathbf{x}\mathbf{x}^H\}$ as the *complex envelope correlation* method. Much of the research in antenna diversity has involved the measurement of power without phase, leading to the *power envelope correlation* $\mathbf{R}_P = \mathrm{E}\{(|\mathbf{x}|^2 - \boldsymbol{\mu}_P)(|\mathbf{x}|^2 - \boldsymbol{\mu}_P)^T\}$, where $\boldsymbol{\mu}_P = \mathrm{E}\{|\mathbf{x}|^2\}$, and $|\cdot|$ is an element-wise absolute value. Interestingly, for a zero-mean complex-normal distribution with covariance $\mathbf{R}$, the power correlation matrix is simply $\mathbf{R}_P = |\mathbf{R}|^2$, where $|\cdot|$ is element-wise absolute value. This can be seen by considering a bivariate complex normal vector $[a_1\ a_2]^T$ with covariance matrix

$$\mathbf{R} = \begin{bmatrix} R_{11} & R_{R,12} - jR_{I,12} \\ R_{R,12} + jR_{I,12} & R_{22} \end{bmatrix}, \quad (6)$$

where all $R_{\{\cdot\}}$ are real scalars, and subscripts R and I correspond to real and imaginary parts, respectively. Letting

$u_k = \mathrm{Re}\{a_k\}$ and $v_k = \mathrm{Im}\{a_k\}$, the complex normal distribution may also be represented by the 4-variate real Gaussian vector $[u_1\ u_2\ v_1\ v_2]^T$ with covariance matrix

$$\mathbf{R}' = \frac{1}{2}\left[\begin{array}{cc|cc} R_{11} & R_{R,12} & 0 & R_{I,12} \\ R_{R,12} & R_{22} & -R_{I,12} & 0 \\ \hline 0 & -R_{I,12} & R_{11} & R_{R,12} \\ R_{I,12} & 0 & R_{R,12} & R_{22} \end{array}\right]. \quad (7)$$

The power correlation of the kth and ℓth elements of the complex normal vector is

$$\begin{aligned} R_{P,k\ell} &= \mathrm{E}\{|a_k|^2|a_\ell|^2\} - \mathrm{E}\{|a_k|^2\}\mathrm{E}\{|a_\ell|^2\} \\ &= \mathrm{E}\{(u_k^2 + v_k^2)(u_\ell^2 + v_\ell^2)\} - 4\mathrm{E}\{u_k^2\}\mathrm{E}\{u_\ell^2\} \\ &= 4\mathrm{E}^2\{u_k u_\ell\} + 4\mathrm{E}^2\{u_k v_\ell\}, \quad (8) \end{aligned}$$

where the identity $\mathrm{E}\{A^2 B^2\} = \mathrm{E}\{A^2\}\mathrm{E}\{B^2\} + 2\mathrm{E}^2\{AB\}$ (true for arbitrary real Gaussian random variables A and B) and the structure of (7) were used. The magnitude squared of the complex envelope correlation is

$$\begin{aligned} |R_{k\ell}|^2 &= |\mathrm{E}\{u_k u_\ell\} + \mathrm{E}\{v_k v_\ell\} \\ &\quad + j(-\mathrm{E}\{u_k v_\ell\} + \mathrm{E}\{v_k u_\ell\})|^2 \\ &= 4\mathrm{E}^2\{u_k u_\ell\} + 4\mathrm{E}^2\{u_k v_\ell\}, \quad (9) \end{aligned}$$

and therefore, $\mathbf{R}_P = |\mathbf{R}|^2$. Thus, for a given power correlation $\mathbf{R}_P$, we have a family of compatible complex envelope correlations. For simplicity, we let $\mathbf{R} = \sqrt{\mathbf{R}_P}$, where $\sqrt{\cdot}$ is element-wise square root, to obtain the complex-normal covariance matrix for a specified power correlation.

III. CHANNEL MEASUREMENTS

Figure 1 depicts the measurement scenario for the data described in this paper. Channel matrices were measured in the Electrical Engineering Building on the Vienna University of Technology Campus at 5.2 GHz [6]. The transmitter consisted of a positionable monopole antenna on a 20x10 xy grid with $\lambda/2$ inter-element spacing. The receiver employed a directional 8-element uniform linear array (ULA) provided by T-Systems Nova GmbH, having 0.4λ inter-element spacing and a 3 dB beamwidth of $120°$. The channel was probed at $N_F=193$ equi-spaced frequency bins spanning 120 MHz of bandwidth. The transmitter assumed a single fixed location in a hallway. The receive array assumed many different locations in several offices connected to this hallway, as well as three possible orientations: (D1) $0°$ (due south), (D2) $-120°$, and (D3) $-240°$. The data set for location X and orientation Y is referred to herein as XY. For each data set, $N_S=130$ channel matrices with $N_T=8$ transmitters and $N_R=8$ receivers were formed by moving a virtual 8-element ULA over the 20x10 grid. The channel matrices for each data set were stacked into a single $N_R N_T \times N_S N_F$ matrix $\mathbf{H}$.

A multivariate complex normal distribution at each location is plausible, since small movement only affects the phases of the multipath components (not the overall multipath structure), leading to small-scale Rayleigh fading. Three complex normal models were considered by specifying three different covariance matrices: (1) full covariance [FC] and separable Kronecker covariance with either (2) complex envelope correlation [KCE] or (3) power envelope correlation [KPE]. The full
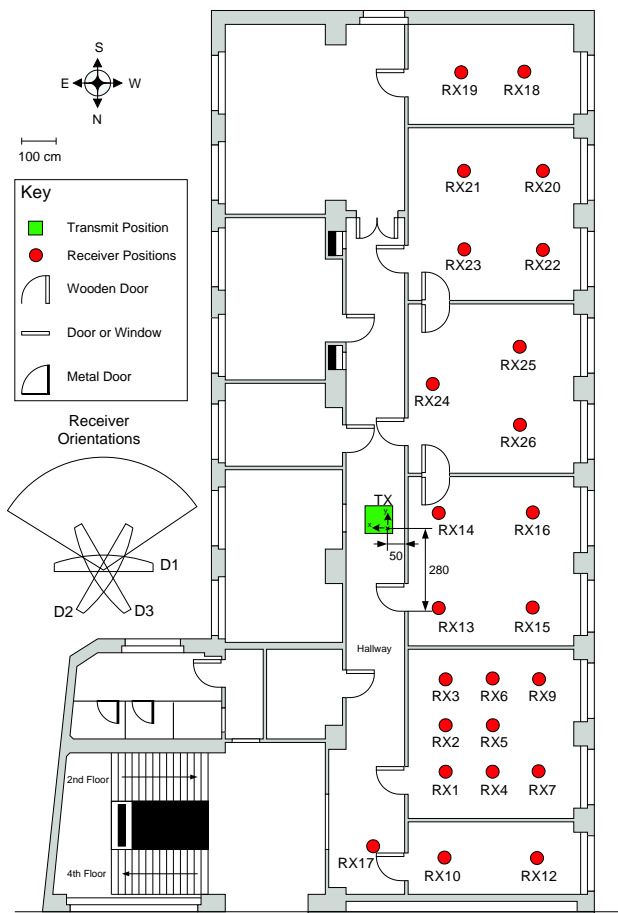
Fig. 1. Measurement Scenario

Fig. 2. Histogram of percent mean absolute error of the spectrum of the KCE model compared to the FC model.

covariance matrix for a fixed receive location was computed by considering each of the N_F frequency bins and N_S channel realizations as samples of a single distribution and computing $\mathbf{R} = (N_S N_F)^{-1} \mathrm{E}\left\{\mathbf{H}\mathbf{H}^H\right\}$. The Kronecker covariance for complex envelope correlation ($\mathbf{R}_K$) was computed from the full covariance according to (3). Finally, the Kronecker covariance for power envelope correlation ($\mathbf{R}_{KP}$) was computed as $\mathbf{R}_{KP} = |\mathbf{R}_K|$.

IV. CAPACITY COMPARISONS

Capacity was computed for each data set with the water-filling solution assuming an average single-input single-output (SISO) SNR of 20 dB. All three of the considered complex normal models produced capacity pdfs that were very close to the capacity pdfs of the actual data. To illustrate accuracy of capacity on a set-by-set basis, average absolute deviation was computed as $\eta = (1/N_S) \sum_{s=1}^{N_S} |c_{M,s} - c_{A,s}|/|c_{A,s}|$, where N_S is the number of data sets and $c_{M,s}$ and $c_{A,s}$ are the modeled and actual mean capacity for data set s, respectively. The percent deviation for the three models was only (1) 0.4%, (2) 2.7%, and (3) 0.6%, indicating that all the complex normal models predict mean capacity reasonably well.

V. JOINT TRANSMIT/RECEIVE BEAMFORMER

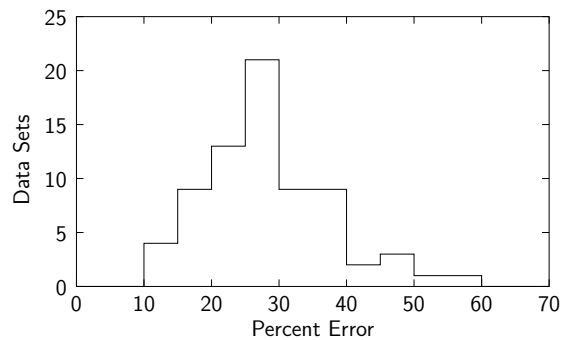Since the complex normal models are able to predict capacity statistics quite well, are all of these channel models good candidates for MIMO channel modeling? We feel that capacity alone is not sufficient to judge the accuracy of a MIMO channel model. Matching capacity only requires matching the behavior of the eigenvalues of the channel, which ignores the structure contained in the eigenvectors. The eigenvectors contain key information about the directional propagation of multipath components, which we refer to as *multipath structure*. If a proposed model does not capture this multipath structure, it may be wholly inadequate for modeling physical antenna systems in realistic propagation scenarios.

To provide a graphical view of the multipath structure described by the various complex normal models, we propose the use of a joint transmit/receive beamformer. We define the joint transmit/receive steering vector $\mathbf{a}(\phi_R, \phi_T)$ as

$$\mathbf{a}(\phi_R, \phi_T) = \mathbf{a}_R(\phi_R) \otimes \mathbf{a}_T(\phi_T), \qquad (10)$$

where the standard separate transmit/receive steering vectors are

$$\mathbf{a}_Q(\phi_Q) = \exp[jk(\mathbf{x}_Q \cos \phi_Q + \mathbf{y}_Q \sin \phi_Q)], \qquad (11)$$

where the ith transmit or receive antenna is located at coordinate $(x_{Q,i}, y_{Q,i})$, k is the free-space wavenumber, and ϕ_R and ϕ_T are receive and transmit azimuth angle, respectively. Many possible beamforming spectra could be considered based on the joint steering vector, but for simplicity, we chose the Fourier spectrum, defined as

$$M(\phi_R, \phi_T) = \mathbf{a}(\phi_R, \phi_T)^H \mathbf{R} \, \mathbf{a}(\phi_R, \phi_T), \qquad (12)$$

which is normalized to obtain a maximum value of unity.

Figure 2 depicts a histogram of the percent absolute mean error of the KCE spectrum compared to the FC (true) spectrum, indicating error ranging from about 10% to 60%. Next we consider three interesting cases, exhibiting the lowest error (11%), typical error (28%), and the largest error (59%).

Figure 3 depicts data set 16D1, exhibiting the smallest deviation of the KCE spectrum. The good match results because only a single transmit direction is important, causing the covariance to be nearly separable. We see also that the KPE model tends to focus the spectrum into a single path, due to the discarding of phase information. Figure 4 shows data set 5D2, a case with more typical error. We see that although the KCE spectrum bears strong similarity to the true FC spectrum, sharp peaks tend to be smoothed out and small artifact peaks are created. Finally, Figure 5 shows data set 13D2, exhibiting
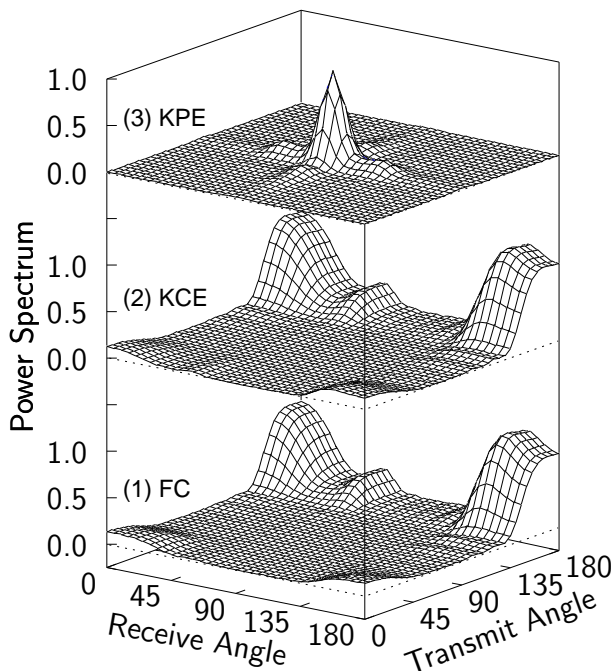
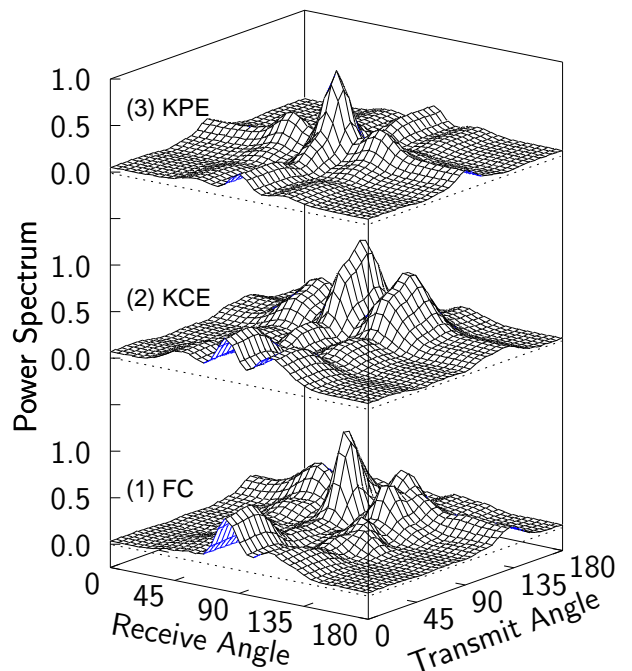Fig. 3. Spectra for the various models for data set 16D1, exhibiting the lowest error.

Fig. 4. Spectra for the various models for data set 5D2, exhibiting typical error.

the poorest match. The true spectrum shows that we have three important propagation paths, and that each transmit direction maps to one and only one receive direction. The KCE spectrum illustrates the main problem with the Kronecker model. By forcing the spectrum to be separable, each transmit direction is coupled with each receive direction, substantially altering the joint spectrum.

These observations lead to two important conclusions regarding the complex normal models. First, for systems with good angular discrimination (many antenna elements), the KCE model may significantly alter the multipath structure present. Second, by discarding phase information, the KPE model fails to retain any of the multipath structure. These conclusions indicate the need for improved complex normal models that represent the detailed multipath structure correctly without the complexity of the FC model.

VI. COVARIANCE GENERATION WITH THE SVA MODEL

In the absence of measurement data, how does one construct realistic covariance matrices? The joint spectra of the indoor data in this paper exhibit between one and five main propagation paths (or clusters of paths), favoring path-based models such as the one presented in [7]. In this section, clusters for each data set are identified with a diffuse estimation technique and combined to estimate the SVA model parameters. The resulting model matches the capacity pdf for the data and generates more realistic joint spectra than standard correlation functions such as Jakes' model.

A. Cluster Estimation

The double-directional channel is a powerful concept for system-independent channel modeling. Usually a discrete response is assumed, meaning that the double-directional chan-

nel response may be written as a sum of propagating plane waves. For the indoor channel, however, these models may be crippled by diffuse scattering mechanisms. Even worse, there may be so many arrivals that the limited temporal and spatial resolution of realistic probing systems prohibits identification of all of the propagation paths, leading to a channel that is effectively diffuse.

The opposite philosophy of assuming discrete arrivals is to assume that the underlying arrivals are diffuse. That is, the directional channel response is characterized by a continuous power spectrum, and under small-scale fading conditions (small movement or frequency sweep), no permanent phase relationship exists between power propagating in distinct directions.

We applied a new diffuse estimation technique (to be treated in a later publication) to obtain cluster parameters for each data set. The key parameters to be obtained from the estimated clusters are the distribution on cluster departure and arrival angle, cluster decay constant (Γ), and cluster angular spread at transmit (σ_T) and receive (σ_R). Cluster departure angle at the transmitter was found to favor propagation down the hallway, and was approximated with a pdf proportional to $|\cos(\theta)|$, with $0°$ as due south. Cluster arrival angle appeared to have little directional preference, and was approximated with a uniform distribution. A simple average was taken of the cluster angular spread at transmit and receive to obtain $\sigma_T = 11°$ and $\sigma_R = 17°$. The cluster decay constant was obtained by considering the three strongest clusters for each location and applying maximum likelihood assuming the Poisson arrival process and exponential cluster decay. This process resulted in $\Gamma = 1.5$.

Figure 6 depicts the capacity pdf of all the measured data compared with the SVA model with the specified extracted
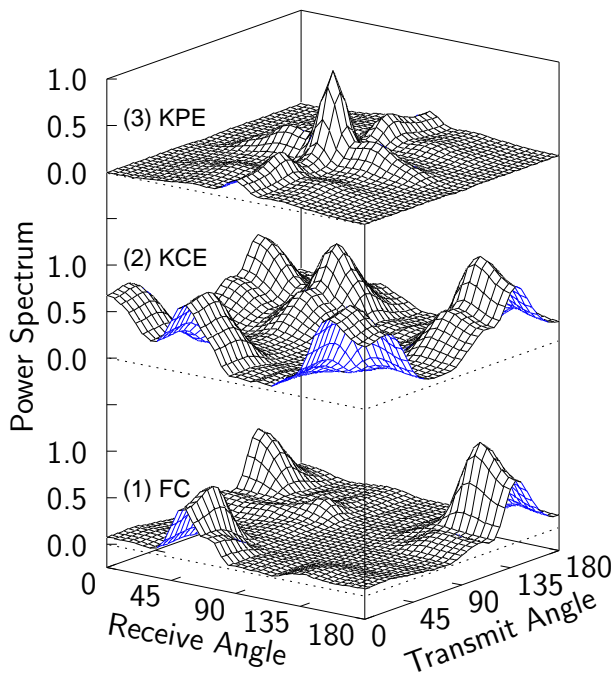
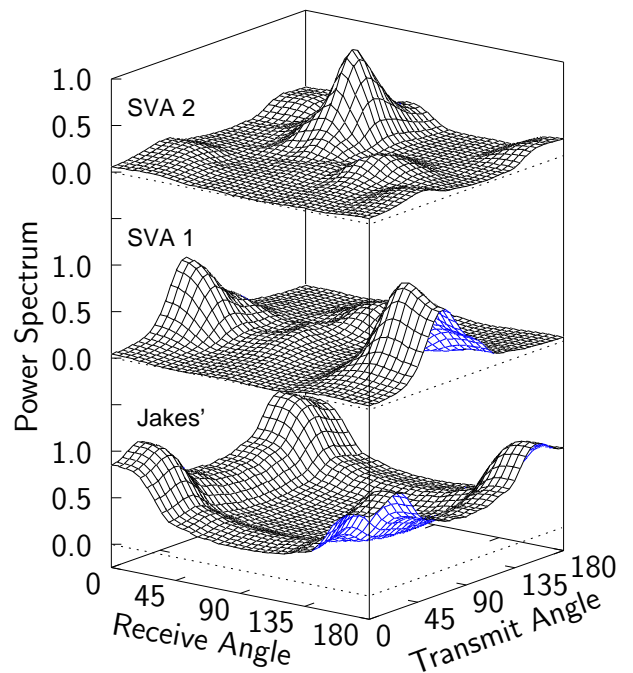Fig. 5. Spectra for the various models for data set 13D2, exhibiting the highest error.
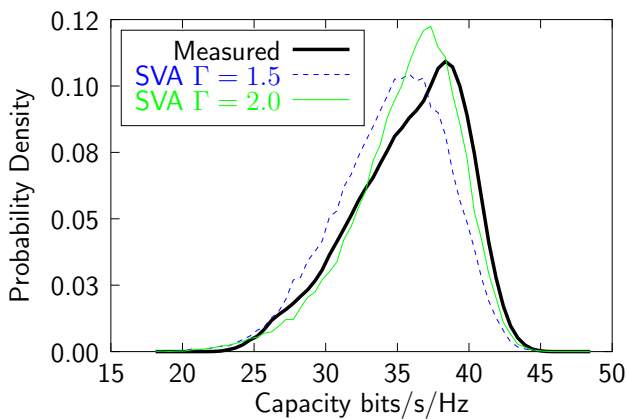

Fig. 6. Capacity pdf of all measured channels and those modeled with the SVA model.

parameters. To improve the capacity fit, the decay constant Γ was increased to 2.0. One of the problems with estimating Γ is that the SVA model generates overlapping clusters, which often look like a single cluster. However, if two clusters were to overlap in the data, the diffuse estimation technique would likely only find a single cluster. Therefore, this estimation method tends to underestimate Γ, and the needed increase is not surprising.

Finally, to demonstrate that the SVA model produces more realistic channel realizations than convenient covariance matrices (Jakes' model, exponential, etc.), Figure 7 plots the joint spectrum of the SVA model and compares with the spectrum for Jakes' model. Jakes' model tends to over-estimate the multipath richness, as indicated in the plot, where significant power is communicated from all transmit directions to all

Fig. 7. Joint spectra for Jakes' model and two random realizations of the SVA model.

receive directions. The two random realizations of the SVA model, on the other hand, look more like spectra obtained from measured channels. Only a few paths, or arrival/departure clusters, support power transfer through the channel.

VII. CONCLUSION

This paper has presented indoor measurements taken at the Vienna University of Technology Campus at 5.2 GHz and applied a joint transmit/receive beamformer to show limitations of the Kronecker model with either complex or power envelope correlation. A diffuse spectrum estimation scheme was used to obtain parameters for the SVA model, which was able to match capacity pdfs of the data and produce realistic joint spectra.

REFERENCES

[1] G. J. Foschini and M. J. Gans, "On limits of wireless communications in a fading environment when using multiple antennas," *Wireless Personal Communications*, vol. 6, pp. 311–335, Mar. 1998.
[2] D. Gesbert, H. Bolcskei, D. A. Gore, and A. J. Paulraj, "Performance evaluation for scattering MIMO channel models," in *ASILOMAR'2000*, Pacific Grove, CA, Oct. 29 - Nov. 1 2000, vol. 1, pp. 738–742.
[3] S. L. Loyka, "Channel capacity of MIMO architecture using the exponential correlation matrix," *IEEE Communications Letters*, vol. 5, pp. 369–371, Sept. 2001.
[4] K. I. Pedersen, J. B. Andersen, J. P. Kermoal, and P. Mogensen, "A stochastic multiple-input-multiple-output radio channel model for evaluation of space-time coding algorithms," in *IEEE VTC'2000 Fall Conf.*, Boston, MA, Sept. 24-28 2000, vol. 2, pp. 893–897.
[5] K. Yu, M. Bengtsson, B. Ottersten, D. McNamara, P. Karlsson, and M. Beach, "Second order statistics of NLOS indoor MIMO channels based on 5.2 GHz measurements," in *IEEE GLOBECOM'01*, San Antonio, TX, Nov. 25-29 2001, vol. 1, pp. 156–160.
[6] M. Herdin, H. Ozcelik, H. Hofstetter, and E. Bonek, "Variation of measured indoor MIMO capacity with receive direction and position at 5.2 GHz," *Electronics Letters*, vol. 38, pp. 1283–1285, Oct. 10 2002.
[7] J. W. Wallace and M. A. Jensen, "Modeling the indoor MIMO wireless channel," *IEEE Transactions on Antennas and Propagation*, vol. 50, pp. 591–599, May 2002.